

1 **Comparing the predictive power of machine learning and semi-mechanistic models of** 2 **endemic measles dynamics**

3 Max SY Lau ^{a,*}, Alex Becker ^b, Lance Waller ^a, Jessica Metcalf ^b, Bryan Grenfell ^b

4 ^a*Department of Biostatistics and Bioinformatics, Rollins School of Public Health, Emory University,*
5 *USA; ^bDepartment of Ecology and Evolutionary Biology, Princeton University, USA*

6
7 * *Corresponding author*

8 **Abstract**

9 Measles is one the best-documented and most-mechanistically-studied non-linear infectious
10 disease dynamical systems. However, systematic investigation into the comparative performance
11 of traditional mechanistic models and machine learning approaches in forecasting the
12 transmission dynamics of this pathogen are still rare. Here, we compare one of the most widely
13 used semi-mechanistic models for measles (TSIR) with a commonly used machine learning
14 approach (LASSO), comparing performance and limits in predicting short to long term outbreak
15 trajectories and seasonality for both regular and less regular measles outbreaks in England and
16 Wales (E&W) and the United States. First, our results indicate that the proposed LASSO model
17 can efficiently use data from multiple major cities and achieve similar short-to-medium term
18 forecasting performance to semi-mechanistic models for E&W epidemics. Second, interestingly,
19 the LASSO model also captures annual to biennial bifurcation of measles epidemics in E&W
20 caused by susceptible response to the late 1940s baby boom. LASSO may also outperform TSIR
21 for predicting less-regular dynamics such as those observed in major cities in US between 1932-
22 45. Although both approaches capture short-term forecasts, accuracy suffers for both methods as
23 we attempt longer-term predictions in highly irregular, post-vaccination outbreaks in E&W.
24 Finally, we illustrate that the LASSO model can both qualitatively and quantitatively reconstruct
25 mechanistic assumptions, notably susceptible dynamics, in the TSIR model. Our results
26 characterize the limits of predictability of infectious disease dynamics for strongly immunizing
27 pathogens with both mechanistic and machine learning models, and identify connections
28 between these two approaches.

29 **Introduction**

30 Mechanistic and semi-mechanistic models have been foundational in developing an
31 understanding of the spread of infectious diseases in human and wildlife populations. These
32 models approximately depict how pathogen transmission is shaped by population dynamics (e.g.,
33 how transmission is reduced by herd immunity). Such modeling approaches are essential for
34 understanding the natural history of pathogens transmission and providing insights into
35 designing effective control strategies. While models such as the Susceptible-Infected-Recovered
36 framework are mechanistically well-understood, calibrating them against stochastic, and often
37 partially unobserved, incidence or mortality data is a steep statistical challenge. The primary
38 focus of mechanistic models has been *understanding and characterizing* the natural history of
39 transmission. In contrast to their mechanistic counterparts, implementations of statistical and
40 machine learning techniques in infectious disease modeling have primarily focused on improving
41 *forecasting* accuracy without the explicit aim of inferring transmission dynamics. Such

42 approaches have grown in popularity in recent years¹⁻⁵, and they also have a long pedigree in
43 terms of using statistical approaches to study measles dynamics^{6,7}.

44 Patterns of pre- and post-vaccination measles incidence are among the most well-documented,
45 and well-studied, non-linear systems in ecology. A suite of analyses using deterministic and
46 stochastic (semi-) mechanistic models have illuminated how the interplay between seasonal
47 forcing and susceptible recruitment shape dynamics in large urban populations⁸, ranging from
48 simple limit cycles to coexisting attractors^{8,9}, and even chaos with the domination of stochastic
49 extinction in small highly vaccinated populations^{10,11}. A focus of previous analysis has been
50 detailed weekly spatio-temporal notifications of measles from England and Wales (E&W),
51 interpreted with the TSIR model and other inferential approaches, notably particle filtering^{12,13}.
52 While partially mechanistic approaches for measles dynamics are being explored¹⁴⁻¹⁶, a more
53 comprehensive comparison between mechanistic and fully statistical approaches is still lacking.
54 Such comparisons would yield insight into the choice of most appropriate modeling techniques
55 given different patterns of data. Measles is an excellent test bed for these questions, given that
56 we have both rich historical notification time series and successful applications of mechanistic
57 and semi-mechanistic models.

58 In this paper, we explore and compare forecasting capability of these two contrasting approaches
59 for both regularly periodic and relatively irregular recurrent measles epidemics in England and
60 Wales between 1944-1994 and in the US between 1932-45. We consider both a stochastic semi-
61 mechanistic TSIR model and a fully-statistical model using a popular machine learning (ML)
62 approach (Least Absolute Shrinkage and Selection Operator, the LASSO).

63 Our results suggest that the proposed LASSO model, compared to the TSIR model, can
64 efficiently use data from multiple major cities and achieve similar short-to-medium term
65 forecasting performance for more regular measles outbreaks in E&W during the pre-vaccination
66 era (1944-1964). Strikingly, even when trained solely on data with an annual cycle, forecasts in
67 our LASSO framework capture the characteristic annual to biennial bifurcation 1950 driven by a
68 decline in birth rates. When important demographic information (such as the birth rate data) is
69 not included, the LASSO model still performs reasonably well, likely due to the fact these
70 dynamics may have been implicitly incorporated within the approach (see Models and Methods).
71 LASSO may also outperform the TSIR for predicting less-regular dynamics such as those
72 observed in major cities in the US between 1932-45. Although both approaches capture short-
73 term forecasts, accuracy suffers for both methods as we attempt longer-term predictions in highly
74 irregular, post-vaccination epidemics in E&W. Overall, our results show that fitting a LASSO
75 model may both qualitatively and quantitatively rediscover major mechanistic assumptions in the
76 TSIR model. These insights inform the limits of predictability, and the connections of both
77 approaches in infectious disease dynamics for fully-immunizing pathogens.

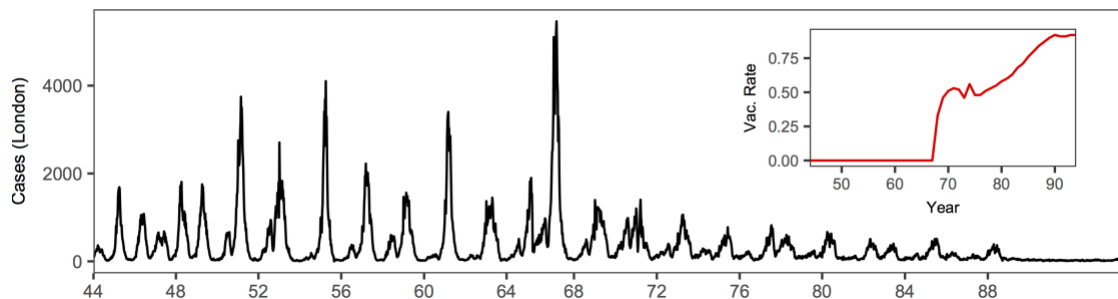
78

79 **Results**

80 **Forecasting measles outbreaks in England and Wales**

81 Measles dynamics pre- and post- the introduction of mass-vaccination program are particularly
82 well-documented from historical notifications in England and Wales¹⁷. Before widespread
83 vaccination in the late 60s, measles epidemics in E&W were characterized by highly regular

84 periodic (often biennial) cycles in large cities (see Figure 1 showing outbreaks in London).
85 Analyses often focus on populations at, or above, the Critical Community Size (i.e., the endemic
86 threshold, CCS) of approximately 300,000 individuals¹⁸. We follow this precedent here and
87 focus on modeling eight major cities, each with a population above the CCS: namely, London,
88 Liverpool, Birmingham, Manchester, Nottingham, Bristol, Leeds and Sheffield. Although
89 dynamics were highly-consistent in the pre-vaccine era, the introduction of measles vaccination
90 in 1968 led to reduction in both epidemic size and regularity.

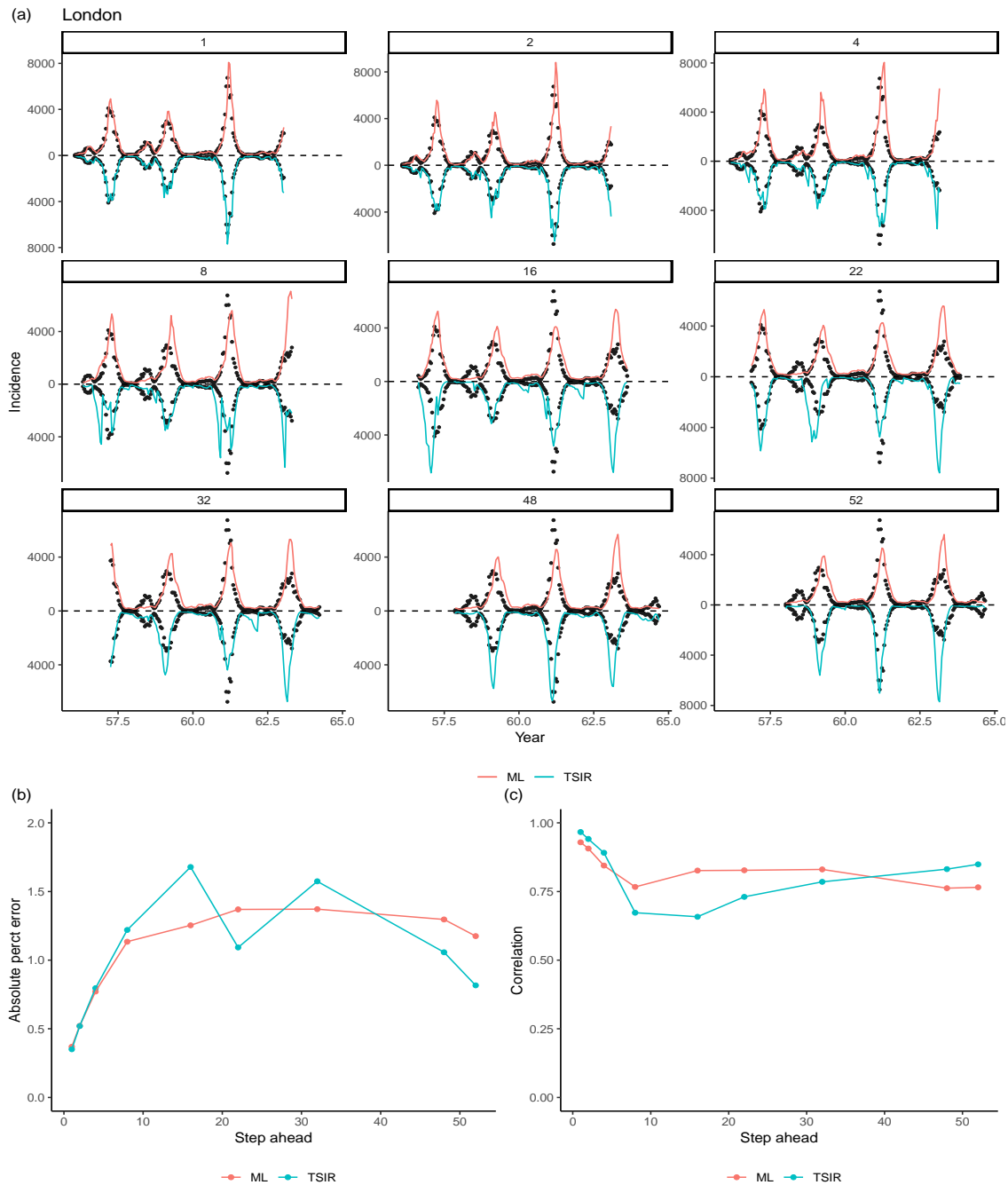


92 *Figure 1: Long-term dynamics of measles in London. Bi-week incidence of measles cases in*
93 *London (1944-94) and time series of vaccination. Following the widespread vaccination in the*
94 *late 60s, the epidemics shifted from highly regular cycles to largely irregular dynamics.*

95 We fit both the LASSO model and the TSIR model (see *Models and Methods*) to the measles
96 epidemics in those major cities in the pre-vaccination era, using the data from 1944-51 for model
97 training. We illustrate our findings by comparing two approaches in predicting epidemics in
98 London. Figure 2 and Figure S1 shows that the TSIR model can predict the epidemic reasonably
99 accurately in short to medium-term. In particular, while both approaches are able to capture the
100 trends of the epidemic trajectories, their accuracy generally decline from 8-biweeks in the future.
101 Although direct inference of a single location (e.g., London) is relatively straightforward in the
102 TSIR framework, incorporating incidence from multiple locations is challenging^{9,17}. The
103 LASSO model, when incorporating all the available incidence data from the major cities, is able
104 to achieve similar performance (Figure S3 also shows that TSIR clearly outperforms LASSO
105 when only London data is used for model training).

106
107 Birth rate is an important variable for mechanistic models including the TSIR model as it
108 governs the rate of the replenishment of susceptible population (see also *Models and Methods*).
109 One common feature of the E&W dataset is an observed bifurcation from annual to
110 predominantly biennial dynamics due to the "Baby Boom" in the late 40s. The impact of this
111 demographic shift was particularly strong; dynamics remained biennial until the transient post-
112 vaccination era starting in the late 60s. We found that the LASSO model forecasts identified and
113 captured the bifurcation reasonably well (Figure 3). Interestingly, we find that the ability of
114 LASSO in predicting the bifurcation remains very similar even without the knowledge of births,
115 the primary causal driver of this dynamic perturbation (Figure S2). By heuristically deriving the
116 connections between TSIR and LASSO (see *Models and Methods*), we show that the impacts of
117 births and susceptibles may have been implicitly incorporated by the LASSO.

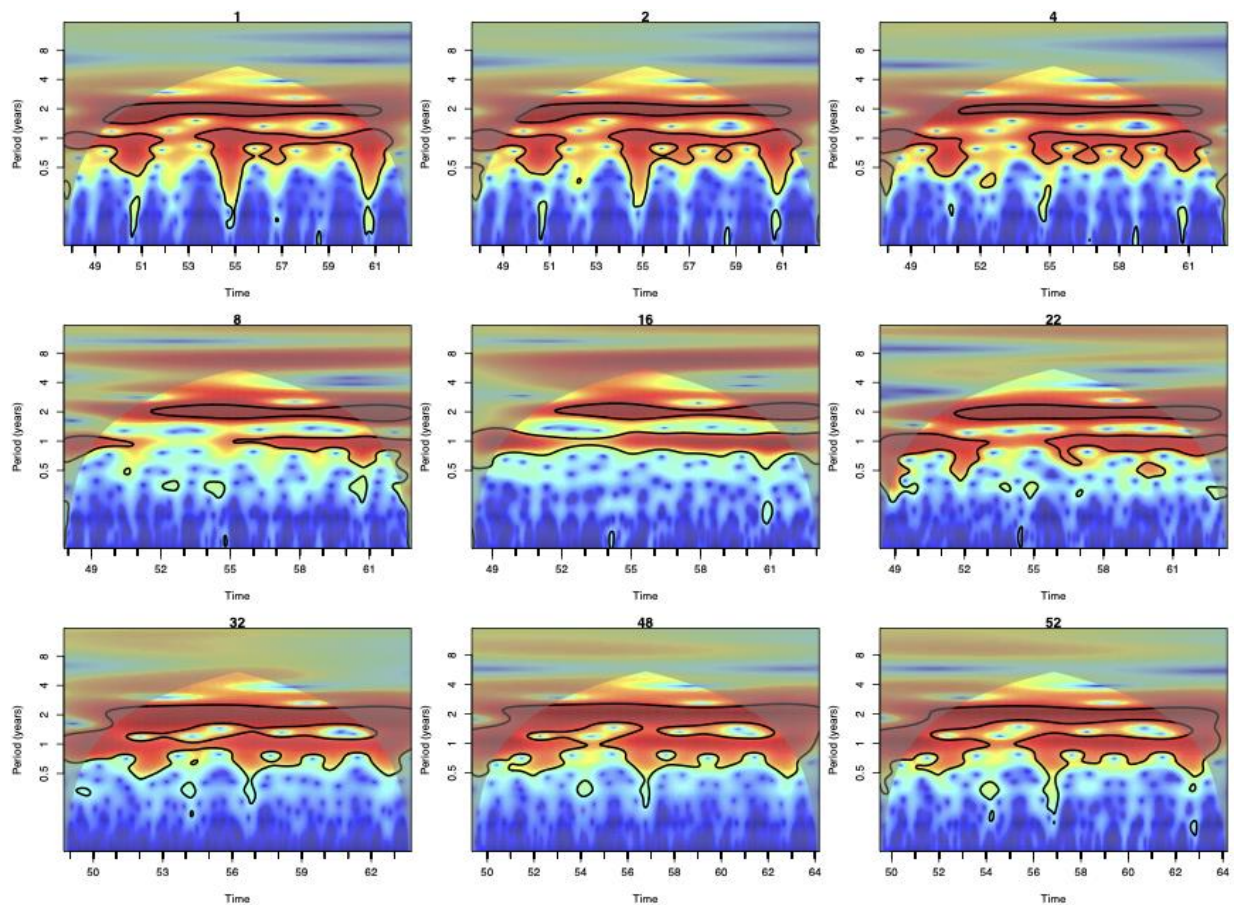
118 Turning to the post-1968 vaccine era, both approaches appear to be able to predict highly
119 irregular epidemic trajectories in the short-term among the highly vaccinated populations, but
120 struggle beyond 4-biweek ahead predictions (Figure 4).



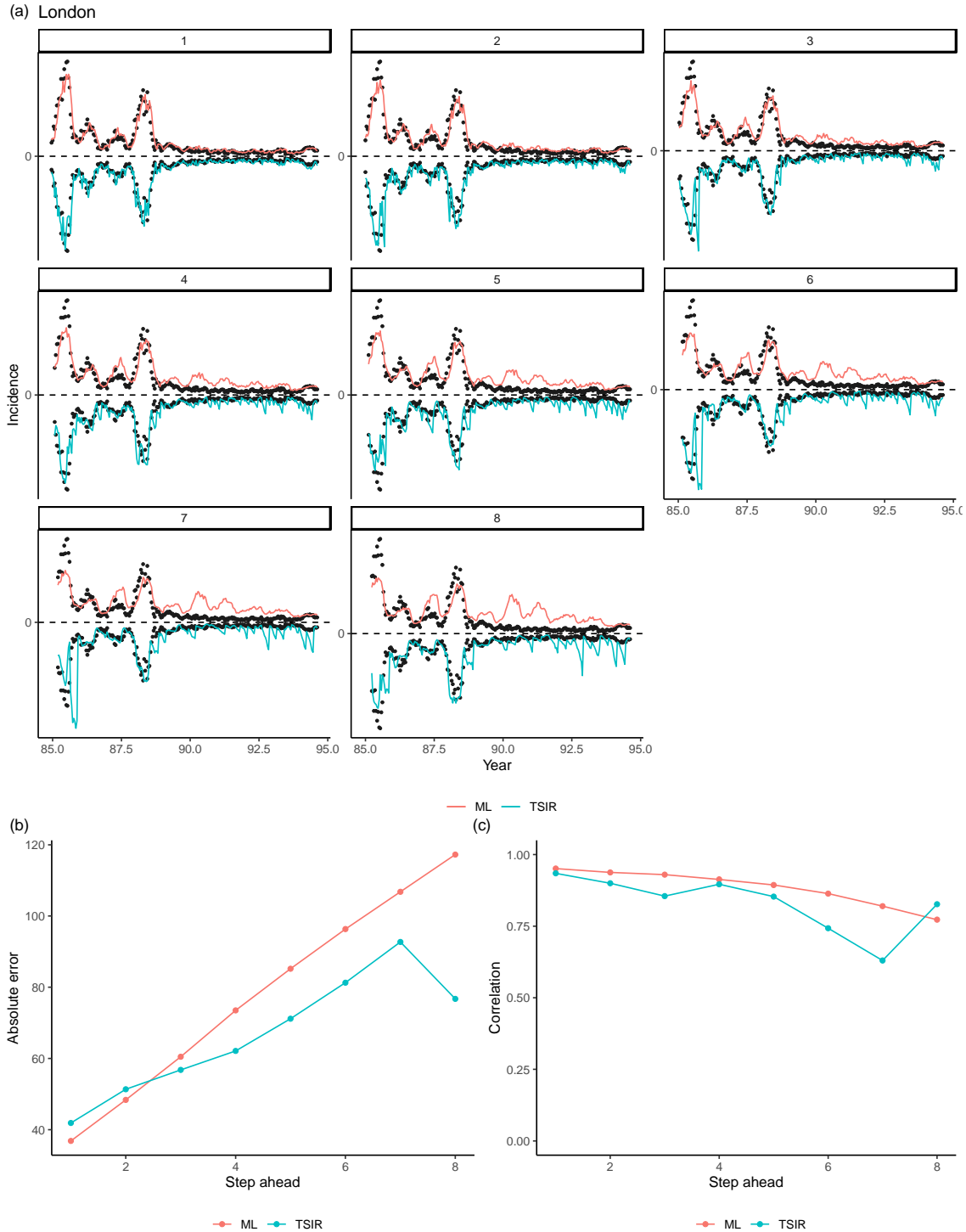
121

122 *Figure 2: Out of sample predictions for measles in London. A subset of 1 to 52th-biweek ahead*
 123 *out-of-sample (i.e., period excluding data in the training set) predictions from our LASSO model*
 124 *and the TSIR model, for pre-vaccination measles epidemics in London from 1944-64. For kth-*
 125 *step ahead predictions, the incidence at a particular time point t was predicted using the LASSO*
 126 *model or TSIR model conditional on observations up between time t - k - t_{lag} and t - k*
 127 *where we use t_{lag} = 130 (see Models and Methods). Data between 1944-51 (from 8 places*
 128 *whose average population sizes are greater than the critical community size 300,000) are used*
 129 *to train a model. Dots indicate the observed incidences. (a) Comparisons of predicted epidemic*
 130 *trajectories; (b) Comparisons of the mean absolute prediction error¹⁹ in ratio (i.e., the absolute*

131 *difference between the predicted and observed value divided by the observed value*); (c)
132 *Comparisons of the trends (summarized by the correlation) between the predicted and observed*
133 *trajectories. Although predictions made by the TSIR appear to be more volatile, performance of*
134 *the two approaches are comparable and they both show the general trend of decreasing*
135 *performance as steps increases.*
136
137
138



139
140 *Figure 3: Power spectra of the out of sample predictions for measles in London using the LASSO*
141 *model. Here we use data between 1944-46 data to train the LASSO models. LASSO successfully*
142 *captures both measles periodicity and bifurcation timing (1950). For each figure, red indicates*
143 *regions of identified periodicity. Black contours indicate 95% confidence intervals. Notably, the*
144 *LASSO model captures the 1950 bifurcation from annual to biennial dynamics starting in 1950.*



145

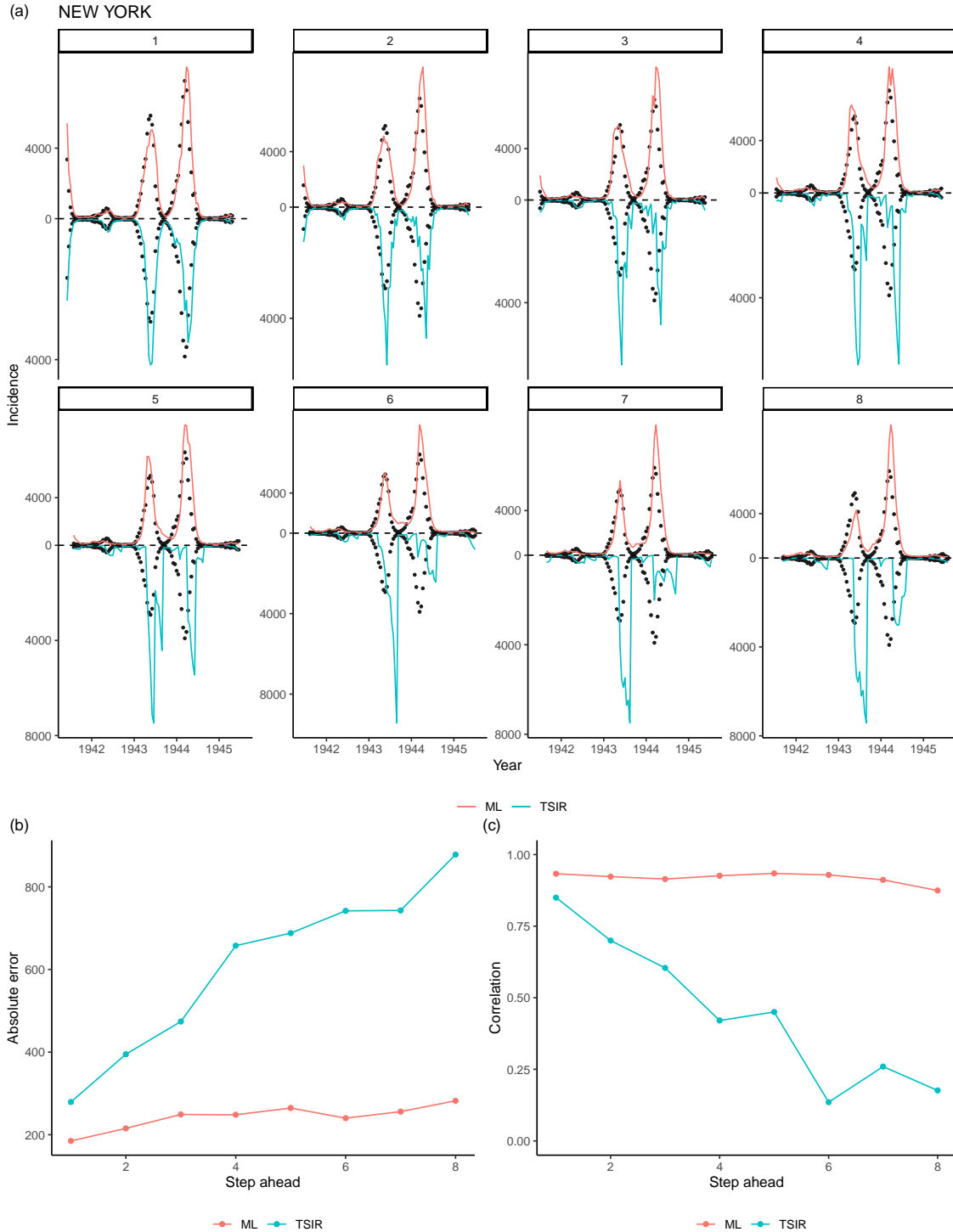
146 *Figure 4: 1 to 8th-biweek ahead out-of-sample predictions from our LASSO model and the TSIR*
 147 *model, for measles epidemics in London during the vaccination era from 1985-94. Data between*
 148 *1970-80 (from 8 places whose average population sizes are greater than the critical community*
 149 *size 300,000) are used to train a LASSO model. Note that here we do not compare the prediction*
 150 *error via a ratio (see Figure 2) because observed incidences (the denominator) are often zero in*

151 *the time period.*

152

153 **Forecasting pre-vaccination measles outbreaks in the US**

154 In the previous section we illustrated how both the TSIR and the LASSO model can successfully
155 capture key traits (e.g., epidemic size and periodicity) of the observed E&W time series data.
156 However, a rich analytical literature has illustrated the relative dynamic stability of the E&W
157 data (i.e., Lyapunov Exponent < 0)^{8,9}. We now turn our attention to a set of incidence data
158 corresponding to more challenging chaotic dynamics (i.e., Lyapunov Exponent > 0). One such
159 source of data comes from the United States. In contrast to E&W, the US city pre-vaccination
160 measles data exhibit signatures of deterministic chaos¹¹. Here, we examine the comparative
161 ability for our LASSO model to predict chaotic dynamics. Fitting both models to the US data, we
162 found the LASSO model may outperform the TSIR model's ability to capture both the amplitude
163 and trend for the outbreak in New York (Figure 5). Similar results can be found for other US
164 major cities (Figure S4).



165

166 *Figure 5: Short-term predictability for irregular dynamics. 1 to 8th-biweek ahead out-of-sample*
 167 *predictions from our LASSO model and the TSIR model, for measles epidemics in New York from*
 168 *1932-45. Data between 1932-40 (from 7 major cities which also have non-missing incidence*
 169 *data during this period) are used to train the LASSO.*

170

171

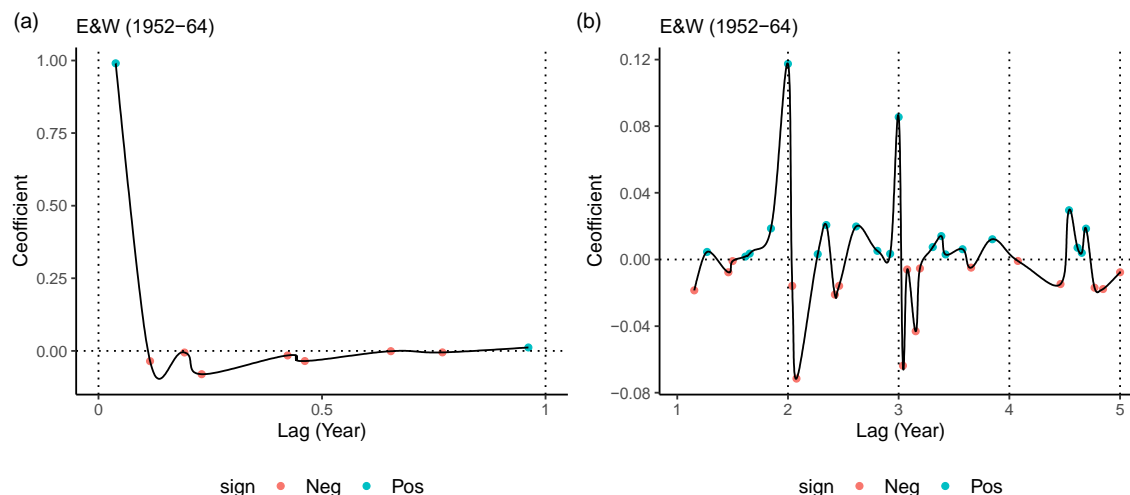
172 Reconstructing the TSIR mechanism via the LASSO model

173
 174 Our E&W results show that our LASSO model may reconstruct/rediscoversome of the
 175 underlying assumptions in the TSIR model. The TSIR model (see also Models and Methods)
 176 assumes that the mean incidence at time t is governed by the product of incidence and S_{t-1} the
 177 number of susceptibles at the previous time step, i.e.,

$$178 \quad E(I_t) = \beta_t I_{t-1}^\alpha S_{t-1},$$

179 where β_t is a seasonally repeating contact rate with 26 biweekly points per year. The exponent α
 180 of the TSIR model captures heterogeneities in mixing, which is typically slightly less than 1
 181 (e.g., 0.98). This formulation implies that I_t is expected to be largely positively associated with
 182 I_{t-1} , and less so with I_{t-k} for $k > 1$ (as larger I_{t-k} in general lead to larger degree of susceptible
 183 depletion and hence smaller S_{t-1}). Secondly, I_t and $I_{t-n \times 26}$ is also expected to have a positive
 184 association due the seasonality assumption embedded in β_t . Our LASSO model estimates appear
 185 to be able to largely capture these trends (i.e., susceptible depletion and seasonality) implied by
 186 the TSIR model (Figure 6). In particular, and our associated LASSO coefficient (of incidence at
 187 the 1-biweek lag) is quantitatively capturing the exponent α in the TSIR model (Figure 6a). We
 188 provide additional insights in the *Models and Methods* regarding how the LASSO model and the
 189 TSIR model are interconnected.

190



191
 192 *Figure 6: Coefficients associated with lagged incidences in the LASSO model (Equation 4 in*
 193 *Models and Methods), from fitting the one-step ahead model to the pre-vaccination E&W data.*
 194 *Only non-zero LASSO coefficients are shown for clarity. The estimated LASSO model resembles*
 195 *and discovers the TSIR model. (a) Coefficient for the most recent lagged incidence is*
 196 *significantly larger (and positive) and most of the coefficients within one year (26 biweeks) are*
 197 *negative, which is consistent with the TSIR assumptions; moreover, the coefficient of the most*
 198 *recent lag is also quantitatively consistent with the value of the exponent parameter (slightly less*
 199 *than 1) in the TSIR model. (b) Coefficients at 2 and 3-year lags are significantly larger (and*
 200 *positive) compared to coefficients at other lags, consistent with the seasonality assumption of the*
 201 *TSIR model. Coefficient at 1-year does not appear to have a positive association, possibly*
 202 *because it is counterbalanced by the effect of susceptible depletion. Lagged incidences beyond 3*

203 *years do not appear to have systematic positive associations.*
204

205 **Discussion**

206 Transmission of infectious diseases at the population-level is characterized by inherent, and often
207 complex, non-linear dynamics that are driven by intrinsic and extrinsic factors such as infectivity
208 of pathogens, human behaviors and public health interventions, notably variable contact patterns
209 and vaccinations among host populations, and even environmental factors. Mechanistic and
210 semi-mechanistic models provide biologically plausible and directly interpretable frameworks
211 for modeling such complex dynamics. In contrast, machine learning approaches primarily focus
212 on identifying patterns within the data to improve prediction and forecasting; they include no
213 specific mechanistic framing, and often lack biological interpretability. While machine learning
214 approaches have shown success in forecasting complex epidemiological systems (e.g., dengue ⁵),
215 comprehensive and long-term data for these pathogen-human interactions are often lacking,
216 making detailed methodological comparisons challenging. Here, we leverage unique time-series
217 data and a large body of work on semi-mechanistic modeling to develop a full comparison
218 between these approaches using measles as a test case.

219 Our results indicate that a LASSO-based machine learning model can efficiently leverage the
220 detailed historical measles incidence data from multiple locations in E&W to achieve short to
221 medium-term forecasting accuracy that is comparable to one of the mostly commonly used
222 mechanistic model for measles (the TSIR model). Interestingly, our results show that the LASSO
223 model performs similarly even without the knowledge of births that are required by the TSIR
224 model. This suggests that the correlation/dependence structure between birth and incidence can
225 be “absorbed” by a parsimonious LASSO model that only considers historical incidence to infer
226 changes in temporal patterns without explicit knowledge of the cause of these changes (e.g.,
227 here, the impact of births on the underlying susceptible population size). As a result, the LASSO
228 model appears to be able to capture the bifurcation in dynamics in 1950, one of the key
229 properties of the measles outbreaks in E&W, without requiring the data driving the change in
230 pattern. We do, however, find that the LASSO forecasts are comparable to those from TSIR only
231 when all data from the major cities are used for model training (Figure S3). Moreover, while
232 both the LASSO model and the TSIR model do not work well for the highly chaotic dynamics
233 beyond short-term prediction, the LASSO approach may outperform TSIR in the scenarios with
234 a mixture of seasonal and mildly chaotic dynamics (as observed in historical outbreaks in the
235 major cities of US ¹¹). Finally, our results also show that the LASSO model can
236 reconstruct/discover the mechanistic assumptions of the TSIR model (Figure 6).

237 Our results are consistent with recent work which shows that the TSIR model may be discovered
238 by some partially-mechanistic machine learning approaches that consider higher orders of
239 polynomial terms for transmission dynamics ¹⁴. Compared to their work, our work focuses on
240 out-of-sample prediction (as opposed to focusing on “discovery”). Also, while these approaches
241 require the knowledge of susceptible population (via some pre-processing procedures leveraging
242 TSIR), we do not require reconstructed susceptible population, creating a more explicit test of
243 fully statistical approaches. The effect of susceptible depletion seems to be implicitly captured by
244 the non-positive LASSO coefficient values associated with the more recent lags within the
245 previous year (see Figure 6a and Models and Methods). This feature is likely to explain why the

246 LASSO model may perform reasonably well despite lacking explicit knowledge of
247 births/susceptibles.

248 This analysis represents an initial step and there are several clear directions for future work:
249 while we compared one of the most successful mechanistic models for measles (the TSIR) with a
250 commonly used machine learning approach (the LASSO), other machine learning approaches
251 (e.g., neural-network based models) may yield different results. In particular, recent theoretical
252 work^{20–22} has demonstrated excellent predictability for simulated deterministic chaotic systems
253 using a network-based machine learning approach (“reservoir computing”). Such variants could
254 also be extended to and tested on the stochastic measles outbreaks that we consider. Despite this,
255 it is worth noting that the LASSO approach is relatively interpretable compared to many other
256 machine learning approaches, and thus seems a sensible starting point here. Finally, while our
257 preliminary simulation studies (Figure S5) further illustrate the predictive power of the LASSO
258 model for measles epidemics, more extensive simulation studies including the investigations of
259 explicitly leveraging spatial information of the epidemics may be considered for future
260 directions. These investigations may shed light on, for example, how machine learning
261 approaches may best complement mechanistic models for modelling less populated places whose
262 dynamics are known to be more stochastically-driven.

263 **Models and Methods**

264 **A mechanistic modelling approach: the TSIR model**

265 We model the local measles dynamics using the time-series-Susceptible-Infected-Recovered
266 (TSIR) framework. Balancing births against disease transmission, the TSIR equations are given
267 as

$$268 \quad E(I_{t+1}) = \beta_{t+1} \times I_t^\alpha \times S_t \quad (1)$$

269 and

$$270 \quad S_{t+1} = B_{t+1} + S_t - I_{t+1} \quad (2),$$

271 Where I_t and S_t are the number of incident and susceptible individuals in a given biweek t , and
272 B_t refers to the number of births in a given biweek, β_t is a seasonally repeating contact rate with
273 26 values per year, and the exponent α (typically slightly less than 1) captures heterogeneities in
274 mixing that were not explicitly modelled by the seasonality^{23,24,14,15} and the effects of
275 discretization of the underlying continuous time process. The TSIR estimates obtained in this
276 manuscript used the recently developed **tsiR** package²⁵. Specifically, in our analysis, α is fixed
277 to be 0.98²⁶ and a Gaussian process regression is performed between cumulative cases and
278 cumulative births. Parameter estimates were obtained for each location for each time period of
279 interest. A more extensive description of the TSIR fitting process in terms of theory and
280 implementation can be found in^{23,25}.

281 **A Machine learning approach: the LASSO model**

282 We consider modelling incidence k -step ahead of time t for place i (i.e., $I_{i,t+k}$) as a linear
283 combination of log-transformed historical local incidence and births. Specifically, we consider

$$284 \quad \log \left(\mathbb{E}(I_{i,t+k}) \right) = \eta + \sum_{j=1}^{T_{lag}} \psi_j \times \log(I_{i,t-j} + 1) + \gamma \times \log \left(\bar{B}_{i,(t-T_{lag}):t} + 1 \right) \quad (4)$$

285 where $\bar{B}_{i,t-T_{lag}:t}$ denotes the average of births of the previous T_{lag} biweeks. We consider bi-
 286 weekly data and two-year forecasting windows $k = 0, 1, \dots, 52$ and $T_{lag} = 130$. A separate
 287 model is fitted for each forecast window k , using Least Absolute Shrinkage and Selection
 288 Operator (LASSO) regression²⁷. LASSO is a machine learning technique that simultaneously
 289 performs estimations of the regression coefficients $\theta = (\eta, \psi_1, \dots, \psi_{T_{lag}}, \gamma)$ and variable
 290 selection by *shrinking* some of the smallest estimated coefficients towards zero. LASSO holds
 291 the property of variable selection as it allows a coefficient to be shrunk to *exactly* zero.
 292 Compared to the traditional regression technique the Least Squares Estimates (LSE), this
 293 shrinkage process has the effect of significantly reducing variance of model prediction and is the
 294 key for improving model fit. We also consider a LASSO model without explicit inclusion of the
 295 births (the last term in Equation 4).

296 In particular, LASSO estimates $\hat{\theta}$ are the values of coefficients that minimize an objective
 297 function

$$298 \quad \sum_{t=1}^n \left(y_{i,t+k} - \eta - \sum_{k=1}^p \theta_k \times x_{t,k} \right)^2 + \lambda \times \sum_{k=1}^p |\theta_k| \quad (5)$$

299 where $y_{i,t+k}$ is the response variable, $p = 2 \times T_{lag}$ and n is the number of observations. Note
 300 that for clarity we have used θ_k to denote the k^{th} coefficient in θ (not including the intercept η)
 301 and $x_{t,k}$ to denote the covariate associated with it. The penalty term $\lambda \times \sum_{k=1}^p |\theta_k|$ serves as the
 302 machinery to allow shrinkage of the coefficient estimates, i.e., the larger the value of λ , the
 303 greater the effect of shrinkage. Shrinkage significantly reduces variances of predictions, but at
 304 the cost of slight increase in bias – and tuning of λ is critical for achieving an ‘optimum’ (often
 305 measured by the test mean squared error) among this bias-variance trade-off. We used ten-fold
 306 cross-validation to identify the optimal value of λ .

307 **Reconstructing the TSIR mechanism via the LASSO model**

308 In this section, we provide additional insights into how our LASSO model can
 309 reconstruct/discover a TSIR model. Taking the log of both sides of TSIR model (Equation 1), we
 310 have

$$\begin{aligned}
 \log(I_{t+1}) &= \log(\beta_{t+1}) + \alpha \times \log(I_t) + \log(S_t) \\
 &= \log(\beta_{t+1}) + \alpha \times \log(I_t) + \log\left\{\sum_{k=1}^{t-1} (B_k - I_k)\right\} \text{ (assuming } S_1 = 0) \\
 &= \log(\beta_{t+1}) + \alpha \times \log(I_t) + \log\left\{\sum_{k=1}^{t-1} B_k - \sum_{k=1}^{t-1} I_k\right\} \\
 311 \quad &= \log(\beta_{t+1}) + \alpha \times \log(I_t) + \log\left\{\sum_{k=1}^{t-1} B_k \times \left(1 - \frac{\sum_{k=1}^{t-1} I_k}{\sum_{k=1}^{t-1} B_k}\right)\right\} \\
 &= \log(\beta_{t+1}) + \alpha \times \log(I_t) + \log\left\{\sum_{k=1}^{t-1} B_k\right\} + \log\left\{1 - \frac{\sum_{k=1}^{t-1} I_k}{\sum_{k=1}^{t-1} B_k}\right\} \\
 &\approx \log(\beta_{t+1}) + \alpha \times \log(I_t) + \log\left\{\sum_{k=1}^{t-1} B_k\right\} - \frac{\sum_{k=1}^{t-1} I_k}{\sum_{k=1}^{t-1} B_k} \text{ (assuming } I_k \text{ is much smaller than } B_k) \\
 &= \log(\beta_{t+1}) + \alpha \times \log(I_t) + c \times \sum_{k=1}^{t-1} I_k + \log\left\{\sum_{k=1}^{t-1} B_k\right\}.
 \end{aligned}$$

312 Note that, under the TSIR, we have $\alpha \geq 0$ (and slightly less than 1) and $c \leq 0$, which
 313 respectively indicate positive association and negative association of the corresponding lagged
 314 incidence I_k with the current incidence. The negative association indicated by the parameter c
 315 may implicitly capture the impact of susceptible depletion. Should the LASSO model (Equation
 316 4) resemble the TSIR, we would expect to see a tendency towards positive coefficients ψ_j
 317 associated with the most recent lagged incidence (corresponding to the positive α value) and
 318 non-positive coefficients at other lagged incidence (corresponding to the non-positive c value).
 319 Also note that historical births may be absorbed in the intercept term of the LASSO model.

320 We stress that we are not aiming to draw close equivalence between the TSIR and our LASSO
 321 model. Instead, this framing aims to provide some insights into the question that how these two
 322 modeling approaches may be interconnected heuristically.
 323

324 References

- 325 1. Dairi, A., Harrou, F., Zeroual, A., Hittawe, M. M. & Sun, Y. Comparative study of machine
 326 learning methods for COVID-19 transmission forecasting. *Journal of Biomedical Informatics*
 327 **118**, 103791 (2021).
- 328 2. Guo, P. *et al.* Developing a dengue forecast model using machine learning: A case study in
 329 China. *PLOS Neglected Tropical Diseases* **11**, e0005973 (2017).
- 330 3. Kim, J. & Ahn, I. Infectious disease outbreak prediction using media articles with machine
 331 learning models. *Sci Rep* **11**, 4413 (2021).

- 332 4. Jiang, F., Zhao, Z. & Shao, X. Time series analysis of COVID-19 infection curve: A change-
333 point perspective. *J Econom* (2020) doi:10.1016/j.jeconom.2020.07.039.
- 334 5. Chen, Y. *et al.* Neighbourhood level real-time forecasting of dengue cases in tropical urban
335 Singapore. *BMC Medicine* **16**, 129 (2018).
- 336 6. Ellner, S. P. *et al.* Noise and Nonlinearity in Measles Epidemics: Combining Mechanistic and
337 Statistical Approaches to Population Modeling. *The American Naturalist* **151**, 425–440
338 (1998).
- 339 7. Olsen, L. F. & Schaffer, W. M. Chaos versus noisy periodicity: alternative hypotheses for
340 childhood epidemics. *Science* **249**, 499–504 (1990).
- 341 8. Grenfell, B. T., Bjørnstad, O. N. & Finkenstädt, B. F. Dynamics of Measles Epidemics:
342 Scaling Noise, Determinism, and Predictability with the Tsir Model. *Ecological Monographs*
343 **72**, 185–202 (2002).
- 344 9. Becker, A. D., Wesolowski, A., Bjørnstad, O. N. & Grenfell, B. T. Long-term dynamics of
345 measles in London: Titrating the impact of wars, the 1918 pandemic, and vaccination. *PLOS*
346 *Computational Biology* **15**, e1007305 (2019).
- 347 10. Ferrari, M. J. *et al.* The dynamics of measles in sub-Saharan Africa. *Nature* **451**, 679–684
348 (2008).
- 349 11. Dalziel, B. D. *et al.* Persistent Chaos of Measles Epidemics in the Prevaccination United
350 States Caused by a Small Change in Seasonal Transmission Patterns. *PLOS Computational*
351 *Biology* **12**, e1004655 (2016).
- 352 12. Ionides, E. L., Bretó, C. & King, A. A. Inference for nonlinear dynamical systems.
353 *Proceedings of the National Academy of Sciences* **103**, 18438–18443 (2006).

- 354 13. King, A. A., Nguyen, D. & Ionides, E. L. Statistical Inference for Partially Observed
355 Markov Processes via the R Package pomp. *J. Stat. Soft.* **69**, (2016).
- 356 14. Horrocks, J. & Bauch, C. T. Algorithmic discovery of dynamic models from infectious
357 disease data. *Sci Rep* **10**, 7061 (2020).
- 358 15. Mangan, N. M., Kutz, J. N., Brunton, S. L. & Proctor, J. L. Model selection for
359 dynamical systems via sparse regression and information criteria. *Proceedings of the Royal*
360 *Society A: Mathematical, Physical and Engineering Sciences* **473**, 20170009 (2017).
- 361 16. Brunton, S. L., Proctor, J. L. & Kutz, J. N. Discovering governing equations from data by
362 sparse identification of nonlinear dynamical systems. *Proceedings of the National Academy of*
363 *Sciences* **113**, 3932–3937 (2016).
- 364 17. Lau, M. S. Y. *et al.* A competing-risks model explains hierarchical spatial coupling of
365 measles epidemics en route to national elimination. *Nature Ecology & Evolution* 1–6 (2020)
366 doi:10.1038/s41559-020-1186-6.
- 367 18. Bartlett, M. S. Measles Periodicity and Community Size. *Journal of the Royal Statistical*
368 *Society. Series A (General)* **120**, 48–70 (1957).
- 369 19. MAPE (mean absolute percentage error)MEAN ABSOLUTE PERCENTAGE ERROR
370 (MAPE). in *Encyclopedia of Production and Manufacturing Management* (ed. Swamidass, P.
371 M.) 462–462 (Springer US, 2000). doi:10.1007/1-4020-0612-8_580.
- 372 20. Pathak, J., Lu, Z., Hunt, B. R., Girvan, M. & Ott, E. Using Machine Learning to
373 Replicate Chaotic Attractors and Calculate Lyapunov Exponents from Data. *Chaos* **27**,
374 121102 (2017).

- 375 21. Pathak, J., Hunt, B., Girvan, M., Lu, Z. & Ott, E. Model-Free Prediction of Large
376 Spatiotemporally Chaotic Systems from Data: A Reservoir Computing Approach. *Phys. Rev.*
377 *Lett.* **120**, 024102 (2018).
- 378 22. Pathak, J. *et al.* Hybrid Forecasting of Chaotic Processes: Using Machine Learning in
379 Conjunction with a Knowledge-Based Model. *Chaos* **28**, 041101 (2018).
- 380 23. Finkenstädt, B. F. & Grenfell, B. T. Time series modelling of childhood diseases: a
381 dynamical systems approach. *Journal of the Royal Statistical Society: Series C (Applied*
382 *Statistics)* **49**, 187–205 (2000).
- 383 24. Bjørnstad, O. N., Finkenstädt, B. F. & Grenfell, B. T. Dynamics of Measles Epidemics:
384 Estimating Scaling of Transmission Rates Using a Time Series Sir Model. *Ecological*
385 *Monographs* **72**, 169–184 (2002).
- 386 25. Becker, A. D. & Grenfell, B. T. tsiR: An R package for time-series Susceptible-Infected-
387 Recovered models of epidemics. *PLOS ONE* **12**, e0185528 (2017).
- 388 27. Tibshirani, R. Regression Shrinkage and Selection via the Lasso. *Journal of the Royal*
389 *Statistical Society. Series B (Methodological)* **58**, 267–288 (1996).
- 390 28. Xia, Y. Measles metapopulation dynamics: a gravity model for epidemiological coupling
391 and dynamics. *AMER NATURALIST* **164**, 267–281 (2004).
- 392 29. Erlander, S. & Stewart, N. F. *The Gravity Model in Transportation Analysis: Theory and*
393 *Extensions.* (VSP, 1990).

394

SI: Comparing the predictive power of machine learning and semi-mechanistic models of endemic measles dynamics

Max SY Lau^a, Alex Becker^b, Lance Waller^a, Jessica Metcalf^b, and Bryan Grenfell^b

^aDepartment of Biostatistics and Bioinformatics, Rollins School of Public Health, Emory University

^bDepartment of Ecology and Evolutionary Biology, Princeton University, USA

Contents

1	Supplementary Figures	1
	Figure S1: Out-of-sample predictions made by the LASSO model for the major cities in E&W.	1
	Figure S2: Power spectra of the out of sample predictions for measles in London using the LASSO model without using birth data.	1
	Figure S3: Out-of-sample predictions made by the LASSO model for London, using only data from London for training.	1
	Figure S4: Out-of-sample predictions made by the LASSO model for the major cities in US.	1
	Figure S5: Simulation studies.	1

1 Supplementary Figures

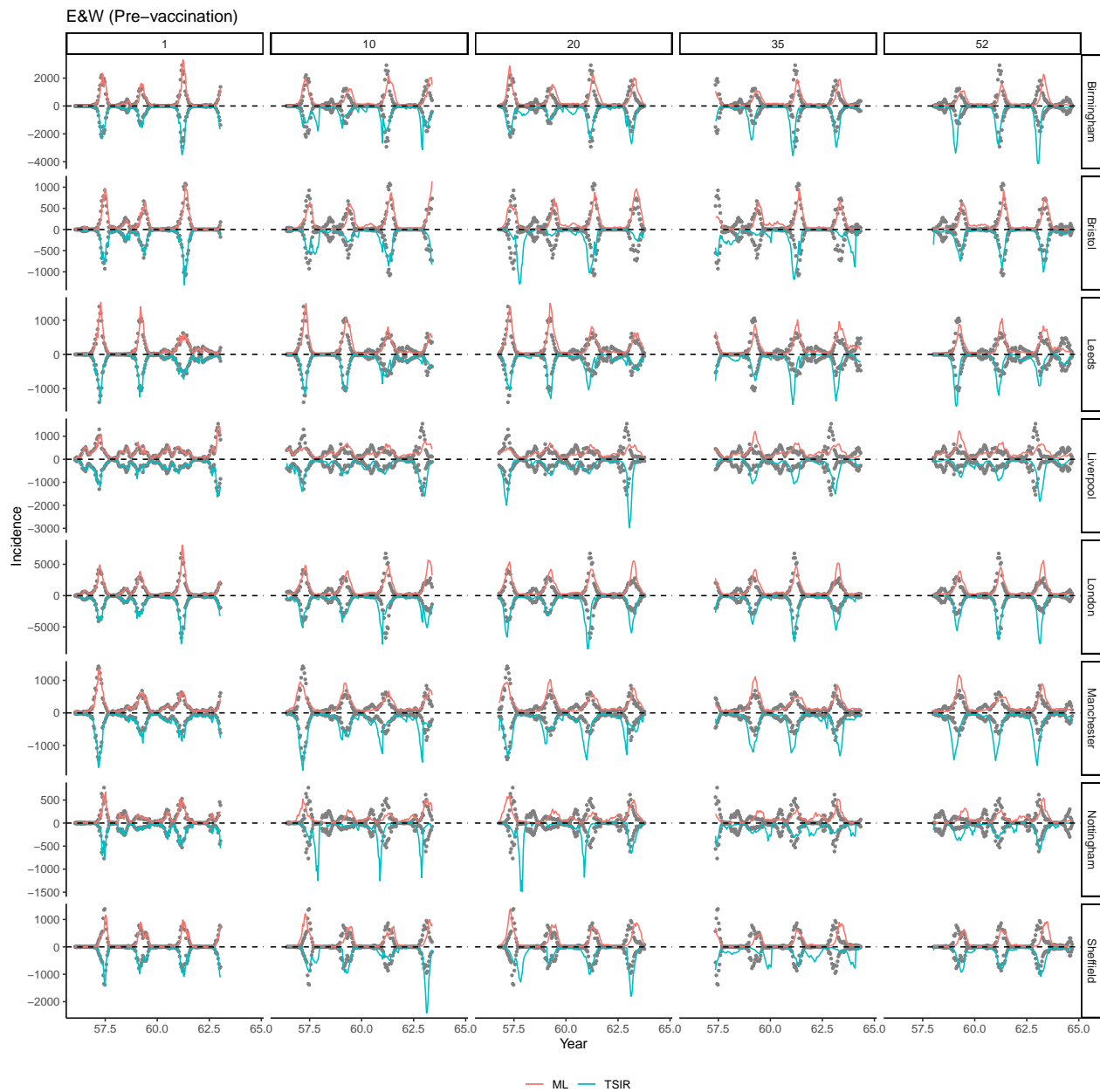


Fig. S1: A subset of 1 to 52th-biweek ahead *out-of-sample* (i.e. period excluding data in the training set) predictions from our LASSO model and the TSIR model, for pre-vaccination measles epidemics in 8 places whose the average population sizes are greater than the critical community size 300,000 from 1944-64.

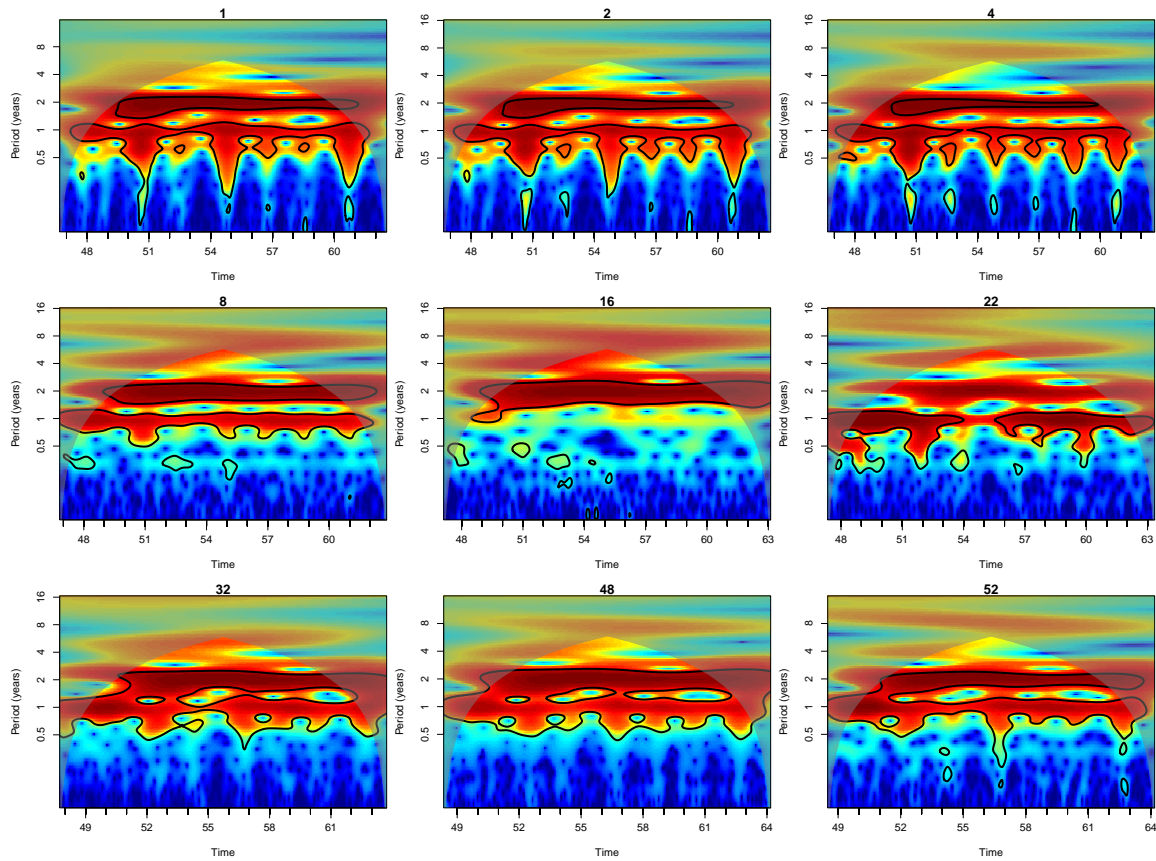


Fig. S2: Power spectra of the out of sample predictions for measles in London using the LASSO model (without using birth data in the LASSO model).

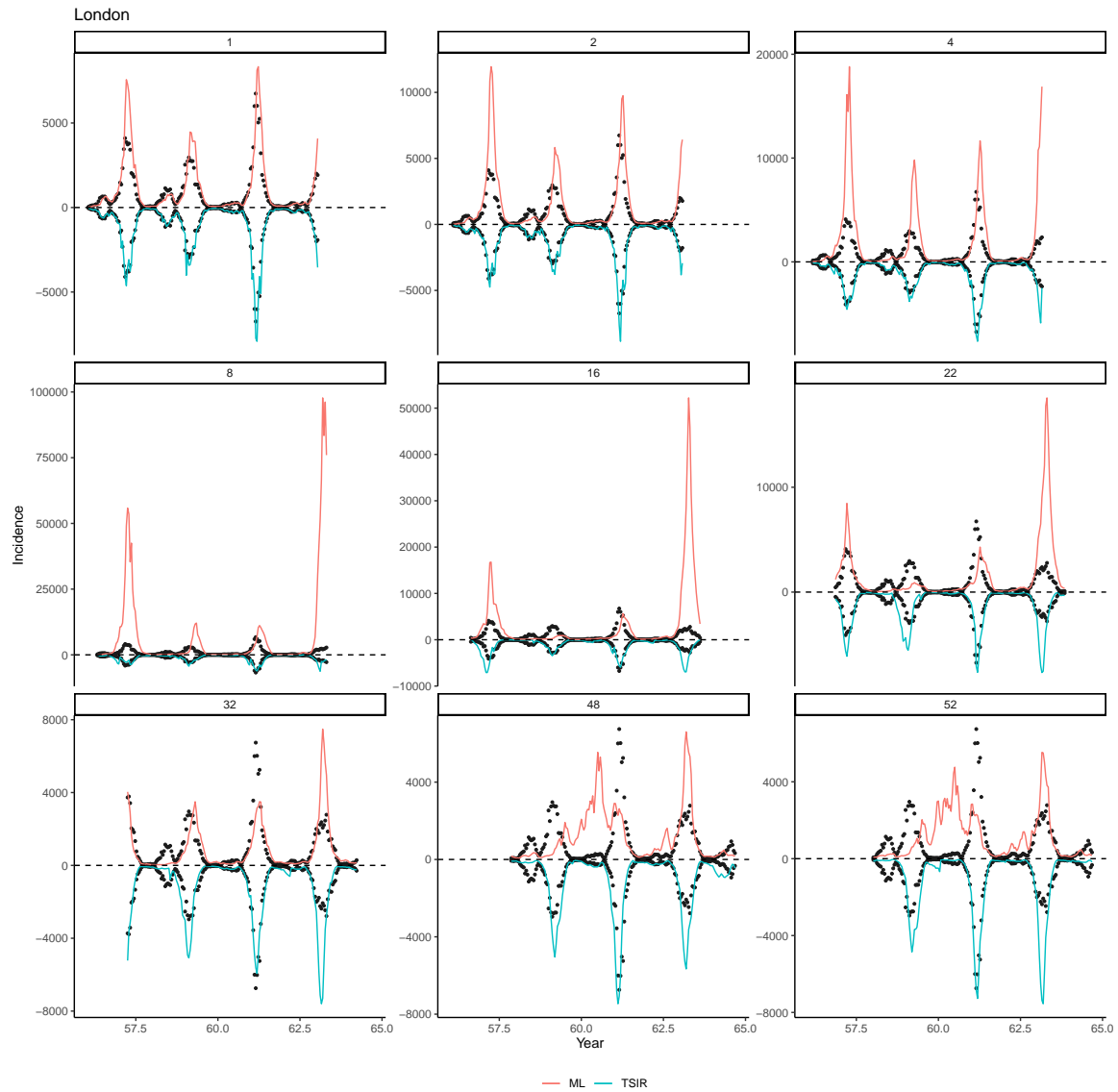


Fig. S3: A subset of 1 to 52th-biweek ahead *out-of-sample* (i.e. period excluding data in the training set) predictions from our LASSO model and the TSIR model, for pre-vaccination measles epidemics in London from 1944-64. Data between 1944-51 (*from London only*) are used to train the LASSO models.

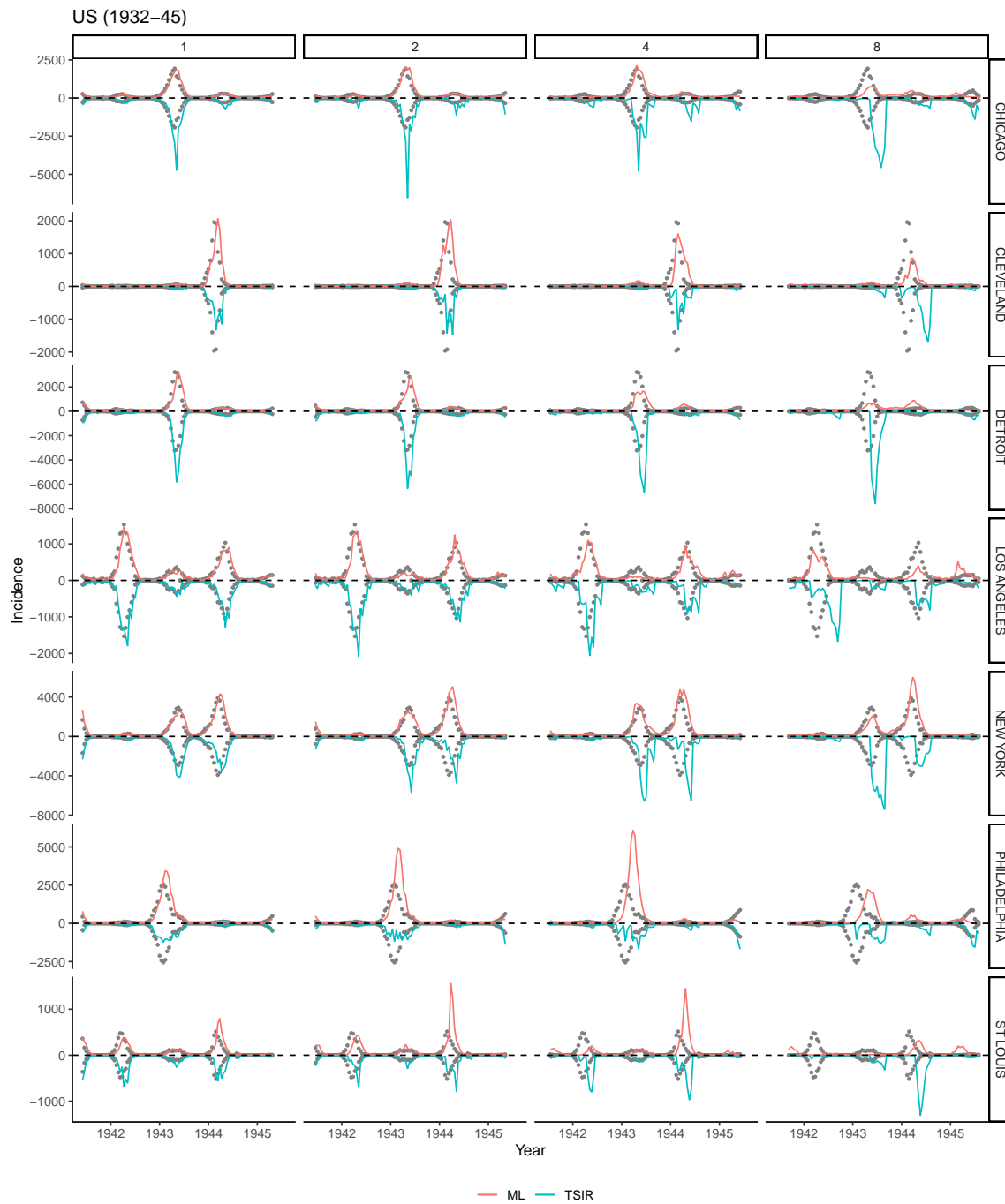


Fig. S4: A subset of 1 to 8th-biweek ahead out-of-sample predictions from our LASSO model and the TSIR model, for measles epidemics in 7 major cities in US from 1932-45. Data between 1932-40 are used to train the LASSO models.

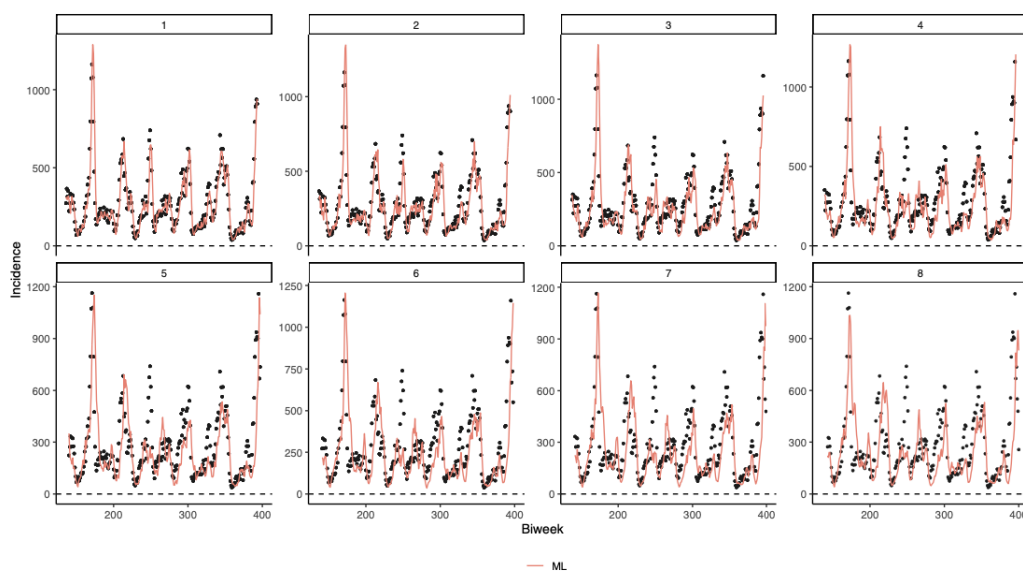


Fig. S5: Simulation studies. Our LASSO model is fitted to epidemics generated from a TSIR model. Specifically, local dynamics are simulated from the estimated TSIR model using the pre-vaccination E&W dataset. Using first half of the data for training, our LASSO model can reasonably well predict the outbreak trajectory.